Int. J. Electrochem. Sci., 14 **(2019)** 8450 – 8469, doi: 10.20964/2019.09.27

International Journal of
ELECTROCHEMICAL
SCIENCE
www.electrochemsci.org

Corrosion Behavior of Common Metals in Eutectic Ionic Liquids

Taleb Hassan Ibrahim[1,*], *Rami Alhasan*[1], *Mohamed Bedrelzaman*[1], *Muhammad Ashraf Sabri*[1], *Nabil Abdel Jabbar*[1], *Farouq Sabri Mjalli*[2]

[1] Department of Chemical Engineering, American University of Sharjah, Sharjah, UAE
[2] Petroleum & Chemical Engineering Department, Sultan Qaboos University, Muscat 123, Oman,
[*]E-mail: italeb@aus.edu

Received: 11 December 2018 / *Accepted:* 1 May 2019 / *Published:* 31 July 2019

The corrosion behavior of six choline chloride-based eutectic solvents namely, ChCl-Ur, ChCl-EG, ChCl-Gl, ChCl-MA, ChCl-Ph and ChCl-TG towards copper, mild steel and stainless steel 316 have been investigated. The effect of temperature and moisture content was evaluated. The corrosion rates of the three materials increased with an increase in the temperature and moisture content. Stainless steel was found to be the most resistant under all experimental conditions. The experimental results demonstrated ChCl-Ph and ChCl-Gl to have high inhibition efficiency suggesting these to be a suitable candidate as green corrosion inhibitors for metal and alloys under extreme environments.

Keywords: Molten salts, Mild steel, Copper, Stainless steel, EIS, Cyclic voltammetry

1. INTRODUCTION

Ionic Liquids (IL) are under considerable industrial attention due to their intrinsic properties of thermal stability, negligible vapor pressure at room temperature, high decomposition temperature, solvation characteristics, non-flammability, and low melting points [1-4]. Ionic liquids have been referred in literature as fused salts, molten salts, ionic fluids, liquid electrolytes, ionic glasses, ionic melts, ambient temperature molten salts, liquid organic salts and designer chemicals [5]. These salts are referred as designer solvents as their physiochemical properties can be easily modified by changing the relevant anions and cations [6-8]. Ionic liquid mixtures, thus, offer enhanced possibilities for fine-tuning of mixture properties according to the desired applications [6-8].

Deep eutectic solvents (DES), a promising subgroup of IL, are eutectic mixtures of Lewis and Bronsted acids and bases. DES generally refers to mixture of salt and hydrogen bond donor to form liquid having melting point lower than its parent components [9, 10]. DES are regarded as alternatives

© 2019 The Authors. Published by ESG (www.electrochemsci.org). This article is an open access article distributed under the terms and conditions of the Creative Commons Attribution license (http://creativecommons.org/licenses/by/4.0/)

to conventional IL and organic solvents due to their cost effectiveness, simple synthesis and flexibility in choice of constituent component [11, 12]. These are frequently being employed for applications in fields such as electrochemistry, solvent extraction, nanotechnology, shape controlled nanosized catalyst synthesis, lubricants and zeolite analogues synthesis [13-18].

Corrosion of metal and alloys is a major concern for industries that leads to financial burden in terms of maintenance and replacement costs. Organic polymeric corrosion inhibitors have conventionally been employed extensively to reduce corrosion of metal and alloys in aggressive media. The use of such corrosion inhibitors is particularly limited due to their low solubility in polar electrolytes, toxicity, non-biodegradability and high volatility. Due to increased environmental concerns associated with conventional corrosion inhibitors, recent studies are focused towards the search for environment benign corrosion inhibitors. IL are being recognized as potential green corrosion inhibitors for metals and alloys on account of their relative non-toxicity, biodegradability and high solubility in polar electrolytes [19-21]. The metal-inhibition bonding and electron rich centers acting as adsorption centers in case of IL is analogous as in case of corrosion inhibition mechanism by traditional organic polymeric inhibiters [5, 21]. The corrosion inhibition efficiency and adsorption behavior of few IL, such as azomethine and indazole derivatives, have been reported in literature [21-23]. Corrosion inhibition efficiency of imidazolium based IL in corrosive media have been reported to increase with an increase in the size and number of alkyl chains [19-22]. However, a longer chain molecule reduces the effective movement of inhibitor molecules in polar media. Thus, a moderate size and chain length is more reasonable in enhancing the corrosion inhibition as it favors the movement of inhibitor molecules from solution to the metallic surface as compared to a longer chain molecule [5, 24, 25]. Verma et al. suggested choline based IL to be the best example of moderate chain length and size molecule offering optimum conditions (hydrophilic or hydrophobic) for metal-inhibition interactions [5].

Choline chloride based DES (CDES), such as ChCl-Ur, represent an important class of IL as they are biodegradable, non-toxic, inexpensive and water soluble [26]. In spite of these environment friendly properties, the use of CDES as corrosion inhibitors is quite limited. Very few reports explaining the corrosion inhibition behavior of CDES have been reported in literature. An investigation of the corrosion rates of metal electrodes in ChCl-EG and proline-lactic acid showed increased stability and decreased corrosion rates of titanium, nickel and iron [27]. Kityk et al. studied the kinetics and corrosion mechanism of mild steel in ChCl-Ur and ChCl-EG [28]. They concluded that the corrosion in these media can lead to accelerated corrosion of mild steel due to the presence of chloride ions [28]. Understanding the corrosion rates of DES, proposed as potential lubricants, is an important factor to be researched for their commercial applicability. Abbott et al. evaluated the corrosion rates of aluminum, nickel and steel in CDES and reported to have significantly reduced corrosion rates in such media [18].

Research on the synthesis and applications of CDES is a relatively new subject, with first reference to its preparation appearing in literature in 2001. With the potential industrial applications of these materials, one of the properties that are crucial to design and selection for materials of construction for the equipment, is the corrosion properties [29, 30]. The present research is an attempt to report the inhibition behavior and characteristics of mild steel, copper and stainless seell 316 in six CDES (ChCl-Ur, ChCl-EG, ChCl-Gl, ChCl-MA, ChCl-Ph and ChCl-TG) and their aqueous solutions at room and elevated temperatures.

2. EXPERIMENTAL PROCEDURES

2.1. Materials

Malonic acid (assay 99% min.), urea (99% min.), glycerol, ethylene glycol and phenol were purchased from LabChem Inc. Triethyene glycol (extra pure) was supplied by SchartauChemie S.A., Spain, respectively. Potentiostat (ACM Instruments - Gill AC), double distilled water (Water Still Aquatron A4000D, UK), precise vacuum oven (Model WOV-30, DAIHAN Scientific Co. Ltd, Korea) fitted with a vacuum pump (Model G-50DA, UlvacKiko, Japan) and hot plate stirrer (MSH-20D, Korea) were used.

2.2. Metal and alloys Composition

Table 1 summarizes the composition of mild and stainless steel. All elements are mentioned other than iron in these alloys

Table 1. Compositional analysis of mild and stainless steel.

	C	Si	Mn	P	S	Cr	Ni	Mo	N
Mild Steel	0.037	0.001	0.151	0.009	0.014	0.017	0.028	0.001	0.003
Stainless Steel	0.021	0.510	0.950	0.033	0.001	16.8	10.0	2.03	0.039

2.3. CDES Preparation:

21.00 g of the salt, Choline Chloride, was mixed with hydrogen bond donors (HBD) i.e. 18.07g urea, 18.67g ethylene glycol, 27.70g glycerol, 15.65g malonic acid, 42.47g phenol and 67.76g triethylene glycol, respectively according to their respective molar ratios mentioned in literature, as given in Table 2. In each case, the mixture was shaken at 400 rpm and 343 K for one to two hours for the formation of stable DES with no apparent precipitation. All chemicals were subjected to vacuum oven for 24 hours at 343 - 353 K to remove moisture. The prepared DES were put in desiccators to avoid any moisture influence before the measurements.

Table 2. Molar ratio for CDES synthesis

CDES (Salt+HBD)	Salt	HBD	Molar Ratio
ChCl-Ur	Choline Chloride	Urea	1:2
ChCl-EG		Ethylene glycol	1:2
ChCl-Gl		Glycerol	1:2
ChCl-MA		Malonic acid	1:1
ChCl-Ph		Phenol	1:3
ChCl-TG		Triethylen glycol	1:3

2.4. Corrosion Tests

A typical 3 electrode cell was used to carry out the electrochemical measurements. A saturated calomel electrode containing potassium chloride was used as reference electrode (RE). The potential of working electrode (WE) was measured with respect to the RE. A platinum wire was used to act as the auxiliary electrode (AE). The platinum wire transmits current through the DES, either to or from the WE. A Gill AC potentiostat was used to connect the three electrodes. Data was recorded from the software coupled with Gill AC potentiostat. The electrodes, with exposed surface area of approximately 7.5 cm^2, were immersed in a 17 mL of CDES aqueous solution. Before the start of the experiment, the electrodes were immersed in solution for 5 minutes to ensure the thermal equilibrium of the system. Electrochemical measurements were performed and recorded using A GILL AC potentiostat. The three metals were tested with six DESs and their aqueous mixture (water wt%: 5% and 10%) at 298 K, 323 K and 348 K, respectively. EIS and potentiodynamic polarization curves were performed and reported.

The electrochemical impedance spectroscopy was carried out between a frequency range of 1000 Hz to 0.1 Hz with a peak to peak amplitude of 20 mV. The potentiodynamic polarization was conduction within the potential range of -150 mV to +150 mV with a sweep rate of 20 mV/min. The cathodic and anodic regions of the generated Tafel plot were scanned from -150 mV to 0 mV and from 0 mV to + 150 mV, respectively.

3. RESULTS AND DISCUSSION

Electrochemical tests, like linear polarization resistance (LPR), potentiodynamic polarization curves, and Electrochemical Impedance Spectroscopy (EIS) provide a convenient, easy and quick measurements for corrosion rates. Since the corrosion phenomena is time dependent the aforementioned tests may not provide an accurate interpretation of the corrosion rate. Gravimetric method, where the metal is put in the media to be tested then actual change in mass is measured, is more accurate in predicting corrosion rate. Nevertheless, the results obtained from electrochemical tests, besides being quick and convenient can be correlated to the actual corrosion rates, and will give a valid comparison between different metals or different mediums.

The three electrochemical tests mentioned above were performed, and their results show good agreements in describing the corrosion rate trend with respect to the investigated parameters. The full results obtained for the effect of six choline chloride based ionic liquids on acidic corrosion of mild steel, copper and stainless steel has been reported in table 1-18 of the Appendix.

3.1 Potentiodynamic Polarization Studies

The potentiodynaic polarization curves (PPC) for cathodic and anodic PPC for copper, mild steel and stainless steel samples recorded in order to determine the electrochemical nature of the inhibitor CDES molecules [31]. The PPC curves for copper at different temperature and water content (wt%)

using ChCl-Ur are presented in figure 1 – 5 while the complete data for other metals and CDES are presented in table 1-18 of the Appendix

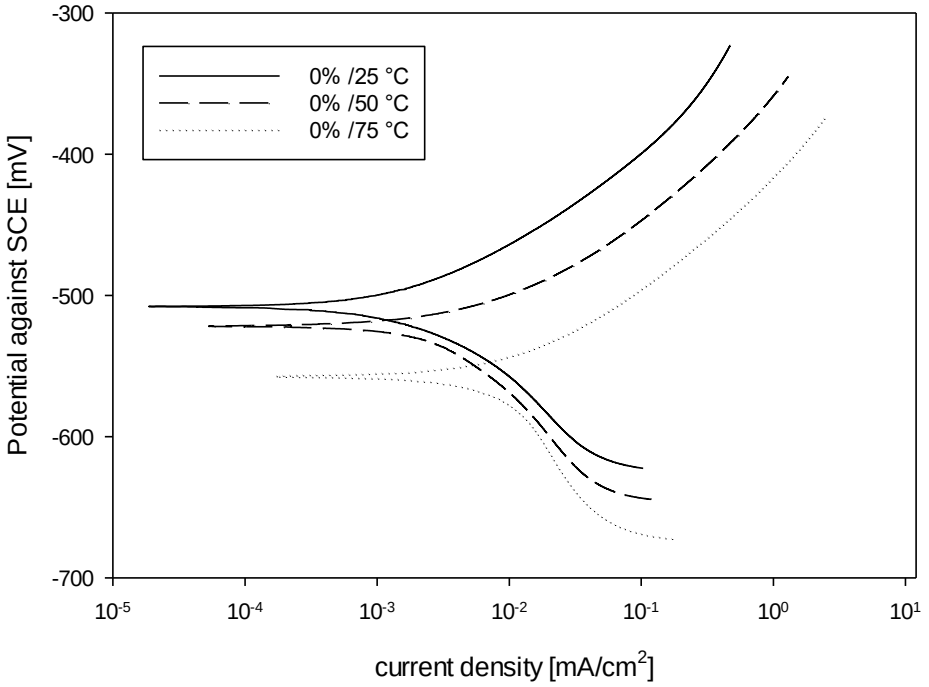

Figure 1. Potentiodynamic polarization curves of copper immersed in pure ChCl-Ur DES (0% water content) at different temperatures

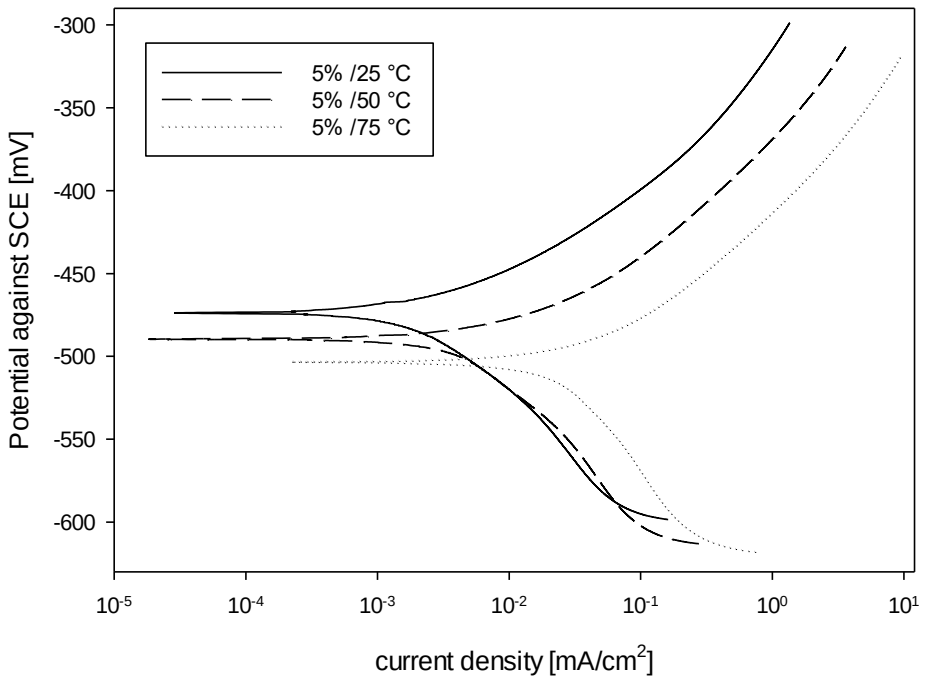

Figure 2. Potentiodynamic polarization curves of copper immersed in ChCl-Ur DES with 5% water content at different temperatures

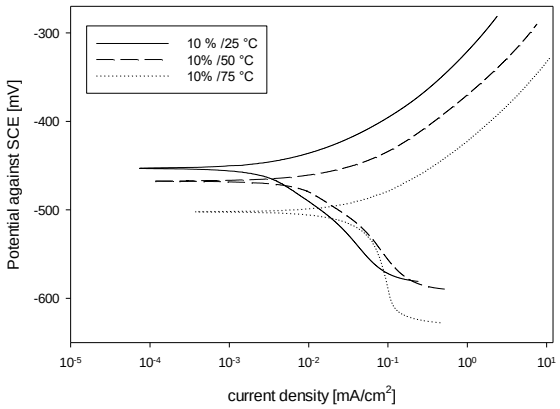

Figure 3. Potentiodynamic polarization curves of copper immersed in ChCl-Ur DES with 10% water content at different temperatures

The data for Copper in ChCl-Ur can be taken as a representative example of the results, the same trend with regards to temperature and water content is observed in the other metals and mediums tested. Figure 1, Figure 2, and Figure 3 show the potentiodynamic polarization curves results for copper in ChCl-Ur at 0% 5% and 10% water content respectively, each figure shows three curves corresponding to different temperatures, namely 25 °C, 50 °C and 75 °C.

The rest potential decreases as temperature increases, this decrease in corrosion potential is cause by a shift in the anodic dissolution of copper, hence the corrosion rate is higher at higher temperatures. A similar trend on the cathodic part of the curve is observed, where the corrosion potential increases as the water content increases, and the increase in potential is accompanied by a shift in the cathodic part of the curve as shown in Figure 4.

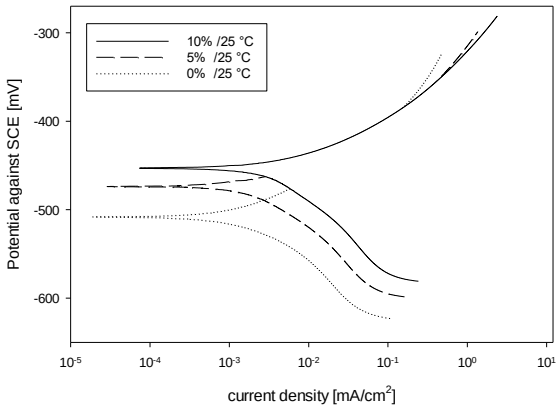

Figure 4. Potentiodynamic polarization curves of copper immersed in ChCl-Ur DES of different water contents at 25 °C

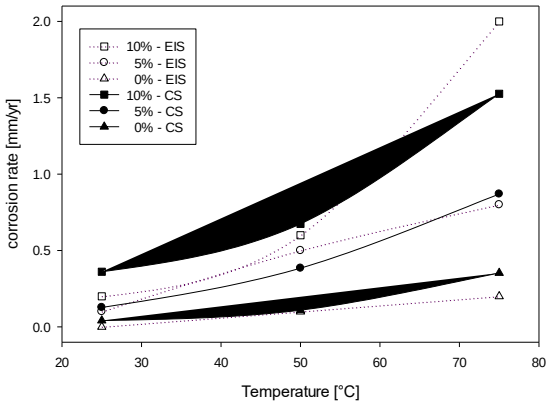

Figure 5. Potentiodynamic polarization curves copper in ChCl-Ur DES at different temperatures and water contents

The values of Tefel parameters from the PPC curves such as slopes (cathodic and anodic), corrosion current density and corrosion potential were determined through extrapolation of linear segments of Tafel cathodic and anodic linear segments. The values of such parameters are presented in table 1-18 of the Appendix

From the results provided in in table 1-18 of the Appendix, it is clear that CDES significantly retards the cathodic and anodic reactions. The significant reduction in the current density in the presence of CDES can be attributed to the adsorption of CDES molecules on the metal surface preventing cathodic or anodic reactions [32, 33].

The corrosion current density increases as the water content in the system increases. It can be seen that increasing the water content at a fixed temperature or increasing the temperature at a fixed water content caused a decrease in the charge transfer resistance R_p and an increase in the double layer capacitance C_{dl}. This indicates that the electrochemical process intermediates from the dissolution of copper have low retention time in this case. The increase in double layer capacitance can be due to a thinner protective film being formed on the copper surface. This can also be attributed to a passive layer formation on the material surface [28]. The displacement of corrosion potential (E_{corr}) in the presence or absence of CDES in the corrosive environment determines the inhibitor type (cathodic, anodic or mixed) [32, 34, 35]. In our present study, both the βc and βa values are affected representing that both metal dissolution (anodic) and hydrogen evolution (cathodic) were inhibited. The inhibition type can be recognized to be cathodic type inhibition as the βc values were more affected compared to βa values [32, 34-37]

3.2 Electrochemical Impedance Spectroscopy (EIS)

The electrochemical impedance spectroscopy is an imperative method to understand the physical processes and electrochemical changes occurring during corrosion of metal at the metal/electrolyte interface [36, 38]. The corrosion characteristics of copper, mild steel and stainless steel in 1 M HCl solution was investigated in six eutectic ionic liquids (pure as well as with 5 – 10 wt% water) at three

different temperatures (25ºC, 50ºC and 75ºC). Figure 6 shows the corrosion rates for copper immersed in 1 M HCl solution with eutectic ionic liquids at various water concentrations (5 – 10 wt%). The results depict that the eutectic ionic liquids act as inhibitor molecules and inhibit corrosion of copper by adsorbing on the material-electrolyte interfaces [31, 39]. Figure 6 show that the presence of water in the solution increases the corrosion rate. The CDES molecules tend to adsorb on the metal/electrolyte surface thus inhibiting corrosion [40]. This suggests that the presence of water in the solution decreases the concentration of the inhibitor in the system and decreases the adsorption of CDES molecules on the metal/electrolyte interface. The decrease in the inhibitor concentration at the metal/electrolyte interface tend to decrease the inhibitive film on the metal surface thus increasing the corrosion rates of copper and other metals.

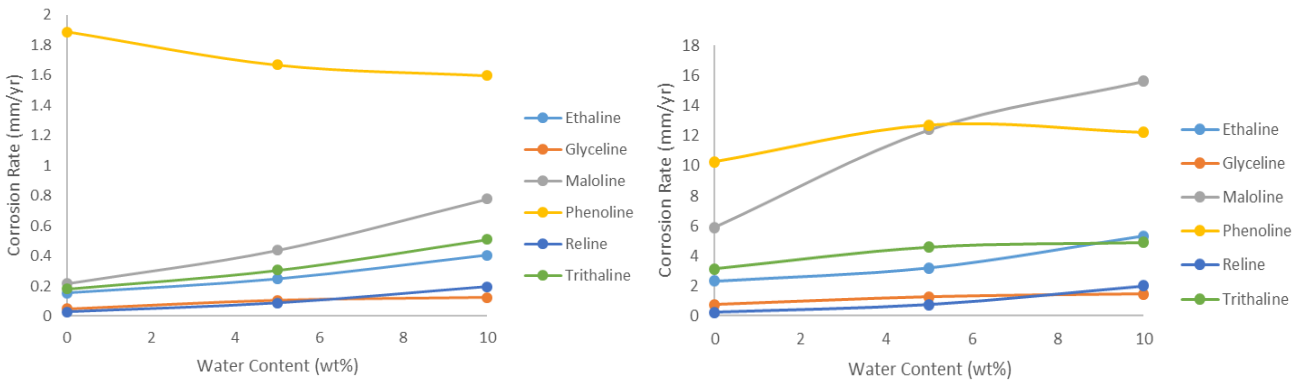

Figure 6. Corrosion rate of copper in CDES with different water contents and at A) 25ºC and B) 75ºC

The analysis of the electrochemical impedance spectra for 1 M HCl medium with pure eutectic ionic liquids and in the presence of water (5-10 wt%) was carried out with the use of suitable equivalent circuit (as shown in figure 6). The values for the solution resistance R_s, the Double layer capacitor C_{dl}, and the polarization resistance R_p, can be obtained and used to interpret the behavior of the system [40, 41]. A Randles circuit with solution resistance R_s, a polarization resistance R_p, and a capacitor C_{dl} as shown in Figure 6, was found to best fit the experimental data from the EIS test [40].

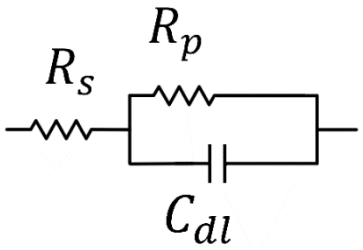

Figure 7. Randles circuit

The main parameters along with the corrosion rates and inhibition efficiencies are provided in table 1-18 of the Appendix

An attempt was made to replace the double layer capacitance by a Constant phase element CPE, in order to compensate for any non-homogeneity in the system which can be caused for instance by roughness in the surface, as opposed to the ideal response from single electrochemical reactions where the capacitor having a phase equal to 1 [42]. The fitting gave less error but the results didn't predict the actual behavior of the system which can be confirmed by the results from potentiodynamic polarization curves. This make it clear that upon fitting a data to a circuit, the best model is not necessary the one with the least error but rather the one that best describes the actual system. Results from the fit to the circuit in Figure 6 are in good accord with the results from the potentiodynamic polarization curves.

Figure 6 presents the corrosion of copper with pure CDES as electrolytes at different temperatures. Inspection of the figure shows that the corrosion of copper increases as the temperature is increased. The maximum inhibition is offered by ChCl-Ur and ChCl-Gl even at elevated temperatures. Similar trends are obvious in case of corrosion of mild steel, copper and stainless steel where the metal corrosion increases with increasing temperature. Similarly, the corrosion rates of mild steel, copper and stainless steel increases with increasing the water content in the solution.

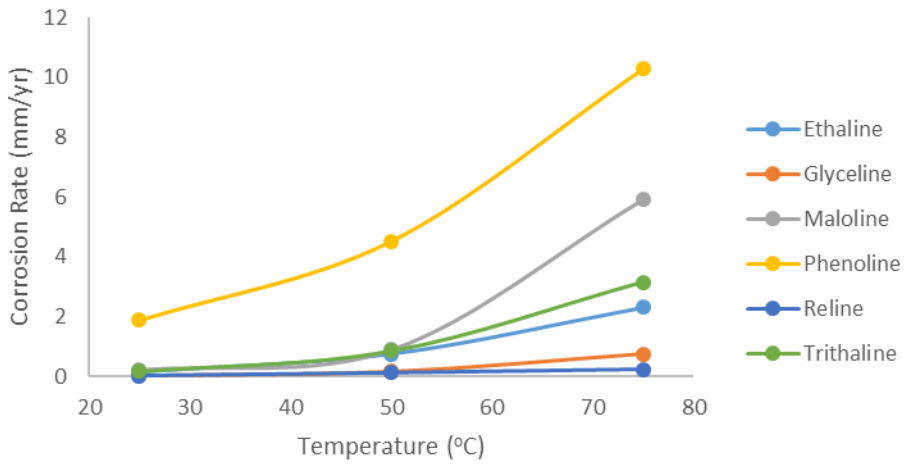

Figure 8. Corrosion rate of copper in pure CDES at different Temperature

The effect of temperature on the corrosion properties of CDES towards copper, mild steel and stainless steel has been shown in Figure 1 to 5 and table 1-18. It is apparent from these tables that the corrosion rates of these materials in CDES increases with increasing the solution temperature. This can be attributed to the high kinetic energies of the CEDS molecules and molecular decomposition of the CDES. The higher kinetic energies of the CDES molecules at high temperatures result in rapid movements that result in decreased attractive forces between CDES molecules and material surface. This increases the desorption probability of the molecules from the material surface resulting in higher corrosion rates of these materials. Furthermore, rapid etching of the material and molecular decomposition of the CDES at elevated temperatures might be attributed to affect the corrosion properties and inhibition efficiency of these CDES resulting in enhanced corrosion rates of mild steel, copper and stainless steel. Similar results have been reported by Verma et al. who used CDES as

corrosion inhibitors on mild steel in acidic media. Additionally, Verma et al. explained in detail the temperature effects on inhibition efficiencies of CDES through Arrhenius equation comparing the activation energies of non-inhibited and inhibited mild steel [5].

It has been established that these CDES are hygroscopic and changes in water contents of the CDES solvents can lead to physicochemical characteristics of these CDES. An increase in the water content in CDES results in decreased viscosity, decreased density and increased conductivity of the CDES-water solution. Thus, an increase in the water content of these CDES effects the physiochemical properties and corrosion activities of CDES on copper, stainless steel and mild steel. Increase in the water content of the CDES results in increased corrosion rates of mild steel, stainless steel and copper. This can be attributed to the reduced viscosity resulting in enhanced diffusion rates. These enhanced diffusion rates can adversely affect the adsorbed CDES protective layer on the material surface. Similar trends were reported by Kityk et al. who reported the mechanism and kinetics of mild steel corrosion in ChCl-EG and ChCl-Ur [28]. Similar studies showing results on the corrosion activities and mechanism of several CDES in acidic environment has been reported in literature [31].

The above results for the corrosion activities of six CDES (ChCl-Ur, ChCl-EG, ChCl-Gl, ChCl-MA, ChCl-Ph and ChCl-TG) on mild steel, stainless steel and copper dictates that two CDES namely ChCl-Ur and ChCl-Gl have lowest corrosion rates for these materials even at elevated temperatures and with moisture content upto 10 wt% percent. This point out towards the fact that these CDES (ChCl-Ur and ChCl-Gl) can be used as corrosion inhibitors in harsh acidic and moist environment for structures and machines related to mild steel, stainless steel and copper.

4. CONCLUSION

In the present study, inhibition effects of six choline based deep eutectic solutions (CDES) has been demonstrated to be effective corrosion inhibitors for copper, mild steel and stainless steel 316. The study reveals that the corrosion rate of these materials increases as the temperature and moisture content increases. The corrosion rate of steel in urea and ethylene glycol based CDES was found to be minimum as compared to other materials and CDES. The corrosion inhibition of stainless steel 316 was found to be maximum in case of pure ChCl-Ur at 25°C. Moreover, the corrosion rate of stainless steel was found to be the lowest at all conditions for urea based CDES materials suggesting it to be suitable for a number of industrial applications. The results suggest that these CDES, urea and glycol based CDES, can be suitable alternatives to traditional organic polymeric corrosion inhibitors.

ACKNOWLEDGEMENT
This work was supported by the American University of Sharjah under grant no. FRG15-R-017.

References

1. Y. Nakata, K. Kohara, K. Matsumoto, and R. Hagiwara, *J. Chem. Eng. Data*, 56 (2011) 1840
2. K.S. Kim, S.Y. Park, S. Choi, and H. Lee, *J. Chem. Eng. Data*, 49, (2004) 1550
3. U. Domańska and A. Marciniak, J. Phys. Chem. B, 112 (2008) 11100
4. U. Domańska, A. Marciniak, M. Królikowska, and M. Arasimowicz, *J. Chem. Eng. Data*, 55 (2010) 2532
5. C. Verma, I. B. Obot, I. Bahadur, E.-S. M. Sherif, and E. E. Ebenso, *Appl. Surf. Sci.,* 457 (2018) 134
6. J. Salgado, T. Regueira, L. Lugo, J. Vijande, J. Fernández, and J. García, *J. Chem. Thermodyn*., 70 (2014) 101
7. M. T. Clough, C. R. Crick, J. Grasvik, P. A. Hunt, H. Niedermeyer, T. Welton and O. P. Whitaker, *Chem. Sci*., 6 (2015) 1101
8. M. Freemantle, *Chem. Eng. News*, 76 (1998) 32
9. A. P. Abbott, G. Capper, D. L. Davies, R. K. Rasheed, and V. Tambyrajah, *Chem. Commun.*, 1 (2003) 70
10. A. P. Abbott, R. C. Harris, K. S. Ryder, C. D'Agostino, L. F. Gladden, and M. D. Mantle, *Green Chem.*, 13 (2011) 82
11. M. A. Kareem, F. S. Mjalli, M. A. Hashim, and I. M. AlNashef, *J. Chem. Eng. Data*, 55 (2010) 4632
12. A. P. Abbott, D. Boothby, G. Capper, D. L. Davies, and R. K. Rasheed, *J. Am. Chem. Soc*., 126 (2004) 9142
13. E. R. Cooper, C. D. Andrews, P. S. Wheatley, P. B. Webb, P. Wormald, and R. E. Morris, *Nature*, 430 (2004) 1012
14. P. Dominguez de Maria and Z. Maugeri, *Curr. Opin. Chem. Biol*., 15 (2011) 220
15. A. Abo-Hamad, M. Hayyan, M. A. AlSaadi, and M. A. Hashim, *Chem. Eng. J.*, 273 (2015) 551
16. M. A. Kareem, F. S. Mjalli, M. A. Hashim, and I. M. AlNashef, " Fluid Phase Equilib., 314 (2012) 52
17. H.G. Liao, Y.X. Jiang, Z.Y. Zhou, S.P. Chen, and S.G. Sun, *Angew. Chem., Int. Ed*., 47 (2008) 9100
18. A. P. Abbott, E. I. Ahmed, R. C. Harris, and K. S. Ryder, *Green Chem*., 16 (2014) 4156
19. J. G. Huddleston, A. E. Visser, W. M. Reichert, H. D. Willauer, G. A. Broker, and R. D. Rogers, *Green Chem*., 3 (2001) 156
20. W. E. S. Hart, J. B. Harper, and L. Aldous, *Green Chem*., 17 (2015) 214
21. C. Verma, E. E. Ebenso, and M. A. Quraishi, *J. Mol. Liq.*, 248 (2017) 927
22. H. Hamani, T. Douadi, D. Daoud, M. Al-Noaimi, and S. Chafaa, *Meas.*, 94 (2016) 837
23. Y. Qiang, S. Zhang, S. Yan, X. Zou, and S. Chen, *Corros. Sci.*, 126 (2017) 295
24. C. Zuriaga-Monroy, R. Oviedo-Roa, L. E. Montiel-Sánchez, A. Vega-Paz, J. Marín-Cruz, and J.-M. Martínez-Magadán, *Ind. Eng. Chem. Res.*, 55 (2016) 3506
25. S. Yesudass, Lukman O. Olasunkanmi, I. Bahadur, M. M. Kabanda, I. B. Obot, and Eno E. Ebenso, *J. Taiwan Inst. Chem. Eng*., 64 (2016) 252
26. D. Rengstl, V. Fischer, and W. Kunz, *Phys. Chem. Chem. Phys*., 16 (2014) 22815
27. D. Di Marino, M. Shalaby, S. Kriescher, and M. Wessling, *Electrochem. Commun.*, 90 (2018) 101
28. A. A. Kityk, Y. D. Rublova, A. Kelm, V. V. Malyshev, N. G. Bannyk, and I. Flis-Kabulska, *J. Electroanal. Chem*., 823 (2018) 234
29. K. Haerens, E. Matthijs, A. Chmielarz, and B. Van der Bruggen, *J. Environ. Manag*., 90 (2009) 3245
30. B. Dilasari, Y. Jung, J. Sohn, S. Kim, and K. Kwon, *Int. J. Electrochem. Sci.*, 11 (2016) 1482
31. R. Solmaz, *Corros. Sci.*, 81 (2014) 75
32. R. Yıldız, T. Doğan, and İ. Dehri, *Corros. Sci.*, 85 (2014) 215
33. R. Fuchs-Godec, *Colloids Surf.,* A, 280 (2006) 130

34. P. Mourya, S. Banerjee, and M. M. Singh, *Corros. Sci.*, 85 (2014) 352
35. C. Verma, M. A. Quraishi, K. Kluza, M. Makowska-Janusik, L. O. Olasunkanmi, and E. E. Ebenso, *Sci. Rep*., 7 (2017) 44432
36. P. Singh, E. E. Ebenso, L. O. Olasunkanmi, I. B. Obot, and M. A. Quraishi, *J. Phys. Chem*. C, 120 (2016) 3408
37. C. Verma, M. A. Quraishi, L. O. Olasunkanmi, and E. E. Ebenso, *RSC Adv.*, 5 (2015) 85417
38. C. Verma, M. A. Quraishi, and A. Singh, *J. Taiwan Inst. Chem. Eng*., 58 (2016) 127
39. M. Chevalier, F. Robert, N. Amusant, M. Traisnel, C. Roos, and M. Lebrini, *Electrochim. Acta,* 131 (2014) 96
40. R. Solmaz, G. Kardaş, M. Çulha, B. Yazıcı, and M. Erbil, *Electrochim. Acta,* 53 (2008) 5941
41. L. R. Chauhan and G. Gunasekaran, *Corros. Sci.*, 49 (2007) 1143
42. M. E. Orazem and B. Tribollet, Electrochemical Impedance Spectroscopy. Wiley, (2011) New Jersey.

Appendix

EIS and CS parameters obtained using Glyceline on copper.
obtained for mild steel in 1 M HCl in absence and presence of different concentrations of GPHs.

Copper:

Table 1. EIS and PPC parameters obtained for Copper in ChCl-EG (in absence and presence of different water content)

T	Water	Rs	CPE-T	Rp	E_{corr}	ba	bc	Corrosion Current	CR-Tafel	CR-EIS
ºC	%	Ω.cm²		Ω.cm²	mV	mV/dec	mV/dec	mA/cm²	mm/yr	mm/yr
25	0	72.02	$1.71*10^{-5}$	1034.00	-464	45.3	103.4	0.01744	0.2021	0.1535
50	0	40.08	$2.88*10^{-5}$	290.50	-467	58.7	169.3	0.05687	0.6591	0.7561
75	0	20.55	$4.00*10^{-5}$	102.00	-499	62.3	189.5	0.16653	1.9302	2.3164
25	5	47.85	$1.87*10^{-5}$	657.40	-447	48.7	93.9	0.03784	0.4386	0.2458
50	5	28.44	$2.94*10^{-5}$	229.80	-465	60.1	191.2	0.08661	1.0039	1.0027
75	5	16.26	$5.09*10^{-5}$	80.46	-484	64.9	241.6	0.19324	2.2398	3.2041
25	10	36.06	$2.09*10^{-5}$	461.90	-429	54.6	115.4	0.04376	0.5072	0.4044
50	10	22.18	$3.51*10^{-5}$	163.70	-449	66.3	267.2	0.12274	1.4226	1.6352
75	10	12.76	$7.83*10^{-5}$	59.39	-464	74.6	391.7	0.27199	3.1525	5.3172

Table 2. EIS and PPC parameters obtained for Copper in ChCl-GI (in absence and presence of different water content)

T	Water	Rs	CPE-T	Rp	E_{corr}	ba	bc	Corrosion Current	CR-Tafel	CR-EIS
ºC	%	Ω.cm²		Ω.cm²	mV	mV/dec	mV/dec	mA/cm²	mm/yr	mm/yr
25	0	414.30	$6.53*10^{-6}$	4028.00	-451	65.9	105.4	0.00603	0.0699	0.0507
50	0	141.40	$2.38*10^{-5}$	1154.00	-481	61.0	121.0	0.01435	0.1663	0.1771
75	0	52.28	$4.50*10^{-5}$	373.70	-516	70.0	254.9	0.03122	0.3619	0.7406
25	5	217.50	$1.22*10^{-5}$	1817.00	-434	60.7	104.1	0.00865	0.1002	0.1063
50	5	77.80	$2.75*10^{-5}$	590.00	-461	57.8	145.7	0.02391	0.2772	0.3535
75	5	30.40	$4.38*10^{-5}$	241.20	-495	71.6	391.2	0.04435	0.5140	1.2645
25	10	117.10	$1.27*10^{-5}$	1397.00	-413	54.8	93.9	0.01788	0.2073	0.1248
50	10	48.83	$3.05*10^{-5}$	387.10	-443	59.7	150.0	0.03548	0.4113	0.5559
75	10	26.59	$5.77*10^{-5}$	210.60	-478	71.8	404.9	0.05112	0.5925	1.4593

Table 3. EIS and PPC parameters obtained for Copper in ChCl-MA (in absence and presence of different water content)

T	Water	Rs	CPE-T	Rp	E_{corr}	ba	bc	Corrosion Current	CR-Tafel	CR-EIS
ºC	%	Ω.cm²		Ω.cm²	mV	mV/dec	mV/dec	mA/cm²	mm/yr	mm/yr
25	0	1078.00	$2.97*10^{-5}$	1025.00	-449	70.1	119.3	0.00743	0.0861	0.2171
50	0	355.90	$8.82*10^{-5}$	302.90	-429	81.4	157.1	0.02983	0.3457	0.8920
75	0	126.80	$2.50*10^{-4}$	70.30	-421	125.6	239.2	0.33317	3.8616	5.9035
25	5	363.20	$1.11*10^{-4}$	483.50	-389	68.9	107.9	0.02665	0.3089	0.4383
50	5	118.40	$2.37*10^{-4}$	125.50	-383	81.6	146.1	0.11952	1.3853	2.1023
75	5	52.82	$2.69*10^{-4}$	31.81	-388	104.8	309.4	0.83284	9.6530	12.4016
25	10	159.90	$2.00*10^{-4}$	266.40	-361	61.8	123.5	0.05716	0.6625	0.7791
50	10	60.50	$2.21*10^{-4}$	66.88	-362	80.4	143.1	0.22076	2.5587	3.8787
75	10	26.35	$3.20*10^{-4}$	22.97	-372	95.4	281.6	1.02547	11.8856	15.6332

Table 4. EIS and PPC parameters obtained for Copper in ChCl-Ph (in absence and presence of different water content)

T	Water	Rs	CPE-T	Rp	E_{corr}	ba	bc	Corrosion Current	CR-Tafel	CR-EIS
ºC	%	Ω.cm²		Ω.cm²	mV	mV/dec	mV/dec	mA/cm²	mm/yr	mm/yr
25	0	7.95	$1.79*10^{-5}$	117.90	-449	70.1	119.3	0.18086	2.0962	1.8873
50	0	6.03	$6.14*10^{-5}$	59.67	-429	81.4	157.1	0.39962	4.6318	4.5282
75	0	4.14	$1.07*10^{-4}$	40.39	-421	125.6	239.2	0.60410	7.0017	10.2752
25	5	9.05	$2.35*10^{-5}$	127.00	-389	68.9	107.9	0.16100	1.8661	1.6685

50	5	6.42	$7.97*10^{-5}$	54.49	-383	81.6	146.1	0.33781	3.9154	4.8421
75	5	3.92	$1.62*10^{-4}$	31.06	-388	104.8	309.4	0.56566	6.5563	12.7010
25	10	9.51	$2.54*10^{-5}$	129.90	-361	61.8	123.5	0.15830	1.8347	1.5979
50	10	6.46	$8.73*10^{-5}$	55.66	-362	80.4	143.1	0.36084	4.1823	4.6606
75	10	3.81	$1.56*10^{-4}$	29.42	-372	95.4	281.6	0.41409	4.7995	12.2058

Table 5. EIS and PPC parameters obtained for Copper in ChCl-Ur (in absence and presence of different water content)

T	Water	Rs	CPE-T	Rp	E_{corr}	ba	bc	Corrosion Current	CR-Tafel	CR-EIS
ºC	%	Ω.cm²		Ω.cm²	mV	mV/dec	mV/dec	mA/cm²	mm/yr	mm/yr
25	0	981.20	$9.14*10^{-6}$	5979.00	-498	57.3	78.3	0.00358	0.0440	0.0279
50	0	177.60	$1.52*10^{-5}$	1559.00	-533	56.6	113.4	0.00945	0.1142	0.1220
75	0	74.30	$1.14*10^{-5}$	1021.00	-547	63.8	164.5	0.03045	0.3285	0.2269
25	5	118.60	$1.44*10^{-5}$	1575.00	-468	41.0	79.2	0.01098	0.1273	0.0864
50	5	44.29	$2.15*10^{-5}$	440.80	-489	58.6	125.5	0.03315	0.3653	0.4567
75	5	32.39	$1.92*10^{-5}$	353.80	-519	66.0	264.1	0.07506	0.9281	0.7521
25	10	47.48	$1.62*10^{-5}$	846.80	-422	44.8	121.0	0.03115	0.3396	0.1946
50	10	26.44	$2.37*10^{-5}$	346.40	-465	56.7	131.7	0.05815	0.6640	0.5766
75	10	17.94	$4.02*10^{-5}$	132.80	-491	66.7	263.5	0.13169	1.4818	2.0198

Table 6. EIS and PPC parameters obtained for Copper in ChCl-TG (in absence and presence of different water content)

T	Water	Rs	CPE-T	Rp	E_{corr}	ba	bc	Corrosion Current	CR-Tafel	CR-EIS
ºC	%	Ω.cm²		Ω.cm²	mV	mV/dec	mV/dec	mA/cm²	mm/yr	mm/yr
25	0	328.60	$2.24*10^{-5}$	1220.00	-488	68.3	121.5	0.01434	0.1662	0.1806
50	0	125.70	$3.18*10^{-5}$	317.10	-494	74.5	197.4	0.05098	0.5909	0.8595
75	0	61.75	$6.25*10^{-5}$	111.50	-506	87.6	334.8	0.12751	1.4779	3.1381
25	5	212.50	$2.78*10^{-5}$	692.80	-465	65.3	117.1	0.02178	0.2524	0.3049
50	5	101.10	$4.09*10^{-5}$	228.10	-471	74.9	247.0	0.06421	0.7442	1.2697
75	5	48.21	$9.43*10^{-5}$	80.16	-483	87.4	443.1	0.16412	1.9022	4.5892
25	10	147.10	$2.97*10^{-5}$	478.90	-446	59.5	11.2	0.02569	0.2978	0.0992
50	10	71.92	$4.84*10^{-5}$	179.00	-456	75.9	272.6	0.07746	0.8978	1.6714
75	10	41.19	$9.18*10^{-5}$	79.14	-471	90.2	517.6	0.17812	2.0645	4.8912

Mild steel:

Table 7. EIS and PPC parameters obtained for mild steel in ChCl-EG (in absence and presence of different water content)

T	Water	Rs	CPE-T	Rp	E_{corr}	ba	bc	Corrosion Current	CR-Tafel	CR-EIS
°C	%	Ω.cm²		Ω.cm²	mV	mV/dec	mV/dec	mA/cm²	mm/yr	mm/yr
25	0	66.93	$5.71*10^{-6}$	19342	-362	53.3	129.5	0.0002	0.0018	0.0099
50	0	37.96	$8.99*10^{-6}$	7330	-385	134.2	113.8	0.0010	0.0113	0.0425
75	0	19.19	$1.89*10^{-5}$	2190	-411	98.4	302.5	0.0039	0.0450	0.1713
25	5	54.06	$9.60*10^{-6}$	10952	-421	54.8	292.2	0.0064	0.0738	0.0213
50	5	29.05	$1.08*10^{-5}$	3872	-429	38.9	195.6	0.0007	0.0079	0.0423
75	5	15.43	$2.68*10^{-5}$	1391	-465	60.3	510.3	0.0075	0.0868	0.1961
25	10	40.38	$1.04*10^{-8}$	8250	-396	47.8	125.3	0.0002	0.0024	0.0212
50	10	17.37	$3.06*10^{-5}$	1737	-435	62.8	298.8	0.0036	0.0419	0.1511
75	10	10.29	$7.93*10^{-5}$	641	-483	61.0	760.1	0.0130	0.1511	0.4452

Table 8. EIS and PPC parameters obtained for mild steel in ChCl-GI (in absence and presence of different water content)

T	Water	Rs	CPE-T	Rp	E_{corr}	ba	bc	Corrosion Current	CR-Tafel	CR-EIS
°C	%	Ω.cm²		Ω.cm²	mV	mV/dec	mV/dec	mA/cm²	mm/yr	mm/yr
25	0	484.6	$1.60*10^{-6}$	55350	-356	70.9	67.4	$6.0*10^{-6}$	$6.7*10^{-5}$	0.0032
50	0	152.6	$4.39*10^{-6}$	12819	-383	46.9	173.0	$1.2*10^{-4}$	$1.4*10^{-3}$	0.0145
75	0	59.83	$9.42*10^{-6}$	3796	-411	42.3	452.2	$5.2*10^{-4}$	$6.0*10^{-3}$	0.0515
25	5	191.7	$5.75*10^{-6}$	17114	-389	56.5	133.4	$4.8*10^{-5}$	$5.6*10^{-4}$	0.0117
50	5	72.39	$6.74*10^{-6}$	6609	-404	44.7	316.8	$4.2*10^{-4}$	$4.8*10^{-4}$	0.0300
75	5	38.56	$1.07*10^{-6}$	2346	-465	53.9	754.2	$1.7*10^{-3}$	$2.0*10^{-2}$	0.1084
25	10	160.3	$5.18*10^{-6}$	13689	-398	57.2	148.8	$1.0*10^{-4}$	$1.2*10^{-3}$	0.0153
50	10	52.48	$1.08*10^{-5}$	4811	-448	42.5	318.2	$4.2*10^{-4}$	$4.8*10^{-3}$	0.0394
75	10	42.78	$8.58*10^{-6}$	1864	-475	48.7	740.7	$2.4*10^{-3}$	$2.8*10^{-2}$	0.1240

Table 9. EIS and PPC parameters obtained for mild steel in ChCl-MA (in absence and presence of different water content)

T	Water	Rs	CPE-T	Rp	E_{corr}	ba	bc	Corrosion Current	CR-Tafel	CR-EIS
°C	%	Ω.cm²		Ω.cm²	mV	mV/dec	mV/dec	mA/cm²	mm/yr	mm/yr
25	0	1643	$2.53*10^{-5}$	2871	-423	113.6	183.7	0.0050	0.0577	0.1236
50	0	498.4	$2.85*10^{-5}$	717.4	-422	152.9	204.2	0.0300	0.3488	0.6159
75	0	146.8	$3.81*10^{-5}$	104.1	-439	218.3	270.9	0.1870	2.1741	5.8693
25	5	550.9	$2.61*10^{-5}$	1861	-414	97.4	166.3	0.0087	0.1015	0.1668
50	5	154.4	$3.13*10^{-5}$	393.5	-430	158.7	230.3	0.0795	0.9243	1.2070
75	5	76.83	$4.26*10^{-5}$	53.88	-433	220.5	246.2	0.3922	4.5597	10.9139
25	10	230.1	$3.36*10^{-5}$	973.4	-421	87.5	141.0	0.0167	0.1942	0.2804
50	10	69.36	$4.00*10^{-5}$	177.5	-430	162.7	209.6	0.1563	1.8171	2.6089
75	10	30.6	$6.83*10^{-5}$	25.43	-429	230.6	241.8	0.9630	11.1959	23.4628

Table 10. EIS and PPC parameters obtained for mild steel in ChCl-Ph (in absence and presence of different water content)

T	Water	Rs	CPE-T	Rp	E_{corr}	ba	bc	Corrosion Current	CR-Tafel	CR-EIS
°C	%	Ω.cm²		Ω.cm²	mV	mV/dec	mV/dec	mA/cm²	mm/yr	mm/yr
25	0	7.043	$2.83*10^{-5}$	915.8	-630	80.2	631.0	0.0251	0.2918	0.3926
50	0	4.544	$5.58*10^{-5}$	381.5	-680	68.6	558.9	0.0447	0.5197	0.8099
75	0	4.085	$1.22*10^{-4}$	162.4	-676	66.1	333.4	0.0880	1.0231	1.7162
25	5	5.282	$3.72*10^{-5}$	631.9	-635	84.0	505.5	0.0135	0.1570	0.5762
50	5	4.628	$1.81*10^{-6}$	334.1	-673	70.2	469.4	0.0475	0.5522	0.9239
75	5	4.31	$9.32*10^{-5}$	201	-680	64.7	312.8	0.0820	0.9533	1.3480
25	10	5.513	$7.47*10^{-5}$	518	-636	70.8	562.1	0.0149	0.1732	0.6132
50	10	4.753	$9.32*10^{-5}$	224.2	-679	68.8	593.1	0.0393	0.4567	1.3891
75	10	3.474	$2.13*10^{-4}$	104.9	-683	67.6	429.9	0.0738	0.8580	2.8141

Table 11. EIS and PPC parameters obtained for mild steel in ChCl-Ur (in absence and presence of different water content)

T	Water	Rs	CPE-T	Rp	E_{corr}	ba	bc	Corrosion Current	CR-Tafel	CR-EIS
°C	%	Ω.cm²		Ω.cm²	mV	mV/dec	mV/dec	mA/cm²	mm/yr	mm/yr
25	0	1094	$1.77*10^{-8}$	2.56E+05	-288	417.4	67.7	$1.0*10^{-6}$	$1.5*10^{-5}$	0.0012
50	0	237.4	$1.80*10^{-6}$	1.31E+05	-154	332.8	61.5	$3.0*10^{-6}$	$3.2*10^{-5}$	0.0020
75	0	90.43	$3.76*10^{-6}$	40036	-158	303.9	87.3	$2.0*10^{-5}$	$2.4*10^{-4}$	0.0086
25	5	110.9	$9.74*10^{-8}$	5.30E+04	-275	471.3	74.5	$3.3*10^{-5}$	$3.8*10^{-4}$	0.0061
50	5	52.92	$6.63*10^{-6}$	23203	-200	537.7	104.8	$3.1*10^{-5}$	$3.6*10^{-4}$	0.0191
75	5	23.46	$7.58*10^{-6}$	3722	-324	218.7	167.9	$2.4*10^{-4}$	$2.8*10^{-3}$	0.1290
25	10	62.82	$5.29*10^{-6}$	26821	-345	202.4	133.8	$1.4*10^{-5}$	$1.6*10^{-4}$	0.0152
50	10	28.25	$1.43*10^{-5}$	3171	-339	263.6	195.5	$1.2*10^{-4}$	$1.4*10^{-3}$	0.1789
75	10	17.07	$1.95*10^{-5}$	1937	-285	885.7	133.4	$3.3*10^{-3}$	$3.8*10^{-2}$	0.3026

Table 12. EIS and PPC parameters obtained for mild steel in ChCl-TG (in absence and presence of different water content)

T	Water	Rs	CPE-T	Rp	E_{corr}	ba	bc	Corrosion Current	CR-Tafel	CR-EIS
°C	%	Ω.cm²		Ω.cm²	mV	mV/dec	mV/dec	mA/cm²	mm/yr	mm/yr
25	0	423.4	$1.36*10^{-5}$	8429	-408	47.4	336.9	0.0002	0.0028	0.0249
50	0	156.3	$3.57*10^{-5}$	2334	-527	63.3	392.1	0.0031	0.0356	0.1180
75	0	72.06	$2.61*10^{-5}$	1677	-595	73.4	437.7	0.0090	0.1044	0.1894
25	5	220	$2.64*10^{-5}$	4511	-523	55.9	314.8	0.0008	0.0096	0.0532
50	5	105.2	$3.13*10^{-5}$	2517	-575	60.1	343.7	0.0039	0.0458	0.1027
75	5	57.73	$3.78*10^{-5}$	985.7	-604	102.5	366.2	0.0124	0.1436	0.4108
25	10	155.2	$4.48*10^{-5}$	4067	-541	58.2	299.4	0.0009	0.0103	0.0606
50	10	75.14	$4.98*10^{-5}$	1780	-579	68.3	356.5	0.0054	0.0630	0.1628
75	10	34.38	$1.42*10^{-5}$	557.6	-601	68.5	433.7	0.0166	0.1925	0.5362

Table 13. EIS and PPC parameters obtained for stainless steel 316 in ChCl-EG (in absence and presence of different water content)

T	Water	Rs	CPE-T	Rp	E_{corr}	ba	bc	Corrosion Current	CR-Tafel	CR-EIS
°C	%	Ω.cm²		Ω.cm²	mV	mV/dec	mV/dec	mA/cm²	mm/yr	mm/yr
25	0	82.9	$1.86*10^{-6}$	31650	-312	106.2	75.7	$1.4*10^{-5}$	$1.6*10^{-4}$	0.0072
50	0	42.5	$6.32*10^{-6}$	18913	-238	64.3	83.8	$1.6*10^{-5}$	$1.9*10^{-4}$	0.0099
75	0	23.3	$1.09*10^{-5}$	7610	-185	100.3	123.9	$2.3*10^{-4}$	$2.7*10^{-3}$	0.0375
25	5	62.3	$3.53*10^{-6}$	30047	-158	143.1	57.6	$6.0*10^{-6}$	$6.6*10^{-5}$	0.0070
50	5	28.4	$5.83*10^{-6}$	22785	-157	65.6	97.6	$0.0*10^{0}$	$0.0*10^{0}$	0.0089
75	5	16.1	$1.31*10^{-5}$	7091	-167	70.8	135.8	$1.5*10^{-5}$	$1.8*10^{-3}$	0.0338
25	10	44.5	$4.69*10^{-6}$	33617	-175	376.7	63.0	$7.0*10^{-6}$	$8.0*10^{-5}$	0.0083
50	10	20.6	$1.29*10^{-5}$	14469	-151	130.6	70.8	$1.1*10^{-5}$	$1.3*10^{-4}$	0.0164
75	10	13.8	$1.17*10^{-5}$	7355	-173	45.7	127.2	$1.9*10^{-4}$	$2.3*10^{-3}$	0.0236

Table 14. EIS and PPC parameters obtained for stainless steel 316 in ChCl-GI (in absence and presence of different water content)

T	Water	Rs	CPE-T	Rp	E_{corr}	ba	bc	Corrosion Current	CR-Tafel	CR-EIS
°C	%	Ω.cm²		Ω.cm²	mV	mV/dec	mV/dec	mA/cm²	mm/yr	mm/yr
25	0	491.2	$2.39*10^{-6}$	35871	-215	228.9	46.6	$8.0*10^{-6}$	$9.3*10^{-5}$	0.0056
50	0	186.9	$3.29*10^{-6}$	17191	-192	65.5	73.2	$2.0*10^{-6}$	$2.6*10^{-5}$	0.0104
75	0	86.3	$7.36*10^{-6}$	6645	-200	60.8	165.8	$1.1*10^{-4}$	$1.2*10^{-3}$	0.0345
25	5	309.1	$2.83*10^{-6}$	17175	-308	505.6	75.4	$1.8*10^{-5}$	$2.1*10^{-4}$	0.0197
50	5	94.1	$4.33*10^{-6}$	10722	-166	77.7	82.0	$1.2*10^{-5}$	$1.5*10^{-4}$	0.0192
75	5	62.9	$1.11*10^{-5}$	5651	-184	52.8	180.7	$1.4*10^{-4}$	$1.6*10^{-3}$	0.0373
25	10	135.7	$6.37*10^{-6}$	13166	-313	821.7	91.7	$2.2*10^{-5}$	$2.6*10^{-4}$	0.0323
50	10	65.7	$1.15*10^{-6}$	9176	-96	115.7	84.0	$7.0*10^{-6}$	$7.9*10^{-5}$	0.0273
75	10	28.3	$1.60*10^{-5}$	5396	-143	87.8	181.3	$1.3*10^{-4}$	$1.6*10^{-3}$	0.0565

Table 15. EIS and PPC parameters obtained for stainless steel 316 in ChCl-MA (in absence and presence of different water content)

T	Water	Rs	CPE-T	Rp	E_{corr}	ba	bc	Corrosion Current	CR-Tafel	CR-EIS
ºC	%	Ω.cm²		Ω.cm²	mV	mV/dec	mV/dec	mA/cm²	mm/yr	mm/yr
25	0	1524.0	$2.43*10^{-5}$	7746	-231	76.0	96.3	0.0004	0.0052	0.0283
50	0	325.3	$3.13*10^{-5}$	4109	-221	76.9	124.5	0.0042	0.0500	0.0596
75	0	123.3	$5.86*10^{-5}$	935	-227	78.2	170.5	0.0227	0.2688	0.2954
25	5	361.9	$3.02*10^{-5}$	6186	-250	82.3	122.6	0.0008	0.0100	0.0410
50	5	110.6	$4.25*10^{-5}$	2184	-240	66.3	141.5	0.0107	0.1264	0.1065
75	5	46.6	$1.00*10^{-4}$	360	-262	57.4	153.6	0.0913	1.0821	0.5990
25	10	144.5	$3.63*10^{-5}$	5034	-256	71.3	113.6	0.0021	0.0250	0.0448
50	10	58.1	$5.09*10^{-5}$	1218	-257	56.6	141.3	0.0249	0.2948	0.1710
75	10	30.1	$1.22*10^{-4}$	230	-280	68.0	157.0	0.1474	1.7472	1.0627

Table 16. EIS and PPC parameters obtained for stainless steel 316 in ChCl-Ph (in absence and presence of different water content)

T	Water	Rs	CPE-T	Rp	E_{corr}	ba	bc	Corrosion Current	CR-Tafel	CR-EIS
ºC	%	Ω.cm²		Ω.cm²	mV	mV/dec	mV/dec	mA/cm²	mm/yr	mm/yr
25	0	7.6	$9.81*10^{-6}$	25100	-123	361.2	87.0	$4.8*10^{-5}$	$5.7*10^{-4}$	0.0144
50	0	5.0	$1.16*10^{-5}$	9320	-106	421.9	81.6	$6.7*10^{-5}$	$7.9*10^{-4}$	0.0378
75	0	5.3	$4.93*10^{-6}$	6874	-76	288.3	86.9	$1.2*10^{-4}$	$1.4*10^{-3}$	0.0501
25	5	7.7	$8.79*10^{-6}$	23967	-121	446.8	70.4	$3.0*10^{-5}$	$3.5*10^{-4}$	0.0131
50	5	4.5	$1.52*10^{-5}$	11340	-99	451.3	128.0	$1.7*10^{-4}$	$2.1*10^{-3}$	0.0453
75	5	4.7	$7.79*10^{-6}$	4195	-74	367.2	76.1	$8.7*10^{-5}$	$1.0*10^{-3}$	0.0775
25	10	10.0	$5.91*10^{-6}$	12817	-122	857.2	67.0	$3.0*10^{-5}$	$3.5*10^{-4}$	0.0250
50	10	7.0	$6.39*10^{-6}$	8023	-95	736.9	91.1	$8.7*10^{-5}$	$1.0*10^{-3}$	0.0521
75	10	5.5	$4.99*10^{-6}$	4525	-71	311.3	103.9	$1.9*10^{-4}$	$2.2*10^{-3}$	0.0887

Table 17. EIS and PPC parameters obtained for stainless steel 316 in ChCl-Ur (in absence and presence of different water content)

T	Water	Rs	CPE-T	Rp	E_{corr}	ba	bc	Corrosion Current	CR-Tafel	CR-EIS
°C	%	Ω.cm²		Ω.cm²	mV	mV/dec	mV/dec	mA/cm²	mm/yr	mm/yr
25	0	995.0	$1.01*10^{-6}$	266760	-294	1564.1	45.8	$8.0*10^{-6}$	$8.9*10^{-5}$	0.0009
50	0	166.2	$2.34*10^{-6}$	62660	-220	606.7	54.8	$1.3*10^{-5}$	$1.6*10^{-4}$	0.0041
75	0	103.9	$2.11*10^{-6}$	23778	-177	423.8	60.3	$1.3*10^{-5}$	$1.5*10^{-4}$	0.0114
25	5	198.6	$1.09*10^{-6}$	207710	-239	591.4	40.8	$4.0*10^{-6}$	$5.3*10^{-5}$	0.0009
50	5	56.8	$7.98*10^{-6}$	16327	-240	600.8	48.5	$7.0*10^{-6}$	$7.8*10^{-5}$	0.0142
75	5	44.7	$2.60*10^{-6}$	14565	-164	378.1	70.5	$3.0*10^{-5}$	$3.4*10^{-4}$	0.0210
25	10	80.1	$6.76*10^{-6}$	16141	-327	570.5	105.2	$8.9*10^{-5}$	$1.1*10^{-3}$	0.0284
50	10	31.9	$3.60*10^{-6}$	15951	-238	487.9	57.8	$1.0*10^{-5}$	$1.2*10^{-4}$	0.0167
75	10	24.4	$2.12*10^{-6}$	10671	-120	344.1	68.7	$3.5*10^{-5}$	$4.1*10^{-4}$	0.0276

Table 18. EIS and PPC parameters obtained for stainless steel 316 in ChCl-TG (in absence and presence of different water content)

T	Water	Rs	CPE-T	Rp	E_{corr}	ba	bc	Corrosion Current	CR-Tafel	CR-EIS
°C	%	Ω.cm²		Ω.cm²	mV	mV/dec	mV/dec	mA/cm²	mm/yr	mm/yr
25	0	445.7	$9.02*10^{-6}$	16604	-146	55.6	146.8	$2.1*10^{-4}$	$2.5*10^{-3}$	0.0125
50	0	156.5	$1.89*10^{-5}$	5084	-146	55.6	146.8	$5.7*10^{-4}$	$6.7*10^{-3}$	0.0409
75	0	80.8	$2.22*10^{-5}$	3505	-156	77.2	333.4	$1.3*10^{-3}$	$1.5*10^{-2}$	0.0922
25	5	272.0	$2.10*10^{-5}$	9587	-57	39.2	103.8	$6.1*10^{-5}$	$7.3*10^{-4}$	0.0153
50	5	107.5	$3.93*10^{-5}$	4827	-68	92.2	258.1	$2.8*10^{-4}$	$3.3*10^{-3}$	0.0725
75	5	60.9	$3.88*10^{-5}$	4426	-126	91.9	283.0	$5.9*10^{-4}$	$7.0*10^{-3}$	0.0808
25	10	213.5	$2.39*10^{-5}$	9786	27	65.7	101.8	$2.6*10^{-5}$	$3.1*10^{-4}$	0.0210
50	10	83.5	$3.75*10^{-5}$	5800	-40	88.3	180.6	$1.9*10^{-4}$	$2.2*10^{-3}$	0.0527
75	10	43.9	$4.09*10^{-5}$	4941	-102	79.6	238.1	$2.8*10^{-4}$	$3.3*10^{-3}$	0.0622

© 2019 The Authors. Published by ESG (www.electrochemsci.org). This article is an open access article distributed under the terms and conditions of the Creative Commons Attribution license (http://creativecommons.org/licenses/by/4.0/).